Eng. Sci., 2021, **14**, 78–93

Engineered Science

DOI: https://dx.doi.org/10.30919/es8d427

Reactions of 2, 3-Dibromonaphthalene-1, 4-Dione and Pyridyl Amines: X-ray Structures, DFT Investigations, and Selective Detection of the Hg^{2+} and Ni^{2+} Ions

Gunjan Aggrwal,[1] Sunita Salunke-Gawali,[1,*] Shridhar P. Gejji,[1] Milind Nikalje,[1] Debamitra Chakravarty,[2] Prakash L. Verma,[1] Prajkta Gosavi-Mirkute,[1] Shital Harihar,[1] Mahesh Jadhav[1] and Vedavati G. Puranik[3]

Abstract

In this work, the products formed by the reaction between 2,3-dibromonaphthalene-1,4-dione with (pyridine-2-yl)methanamine and (pyridine-4-yl)methanamine are discussed in detial. The products 2-amino-3-bromonaphthalene-1,4-dione (**A**) and 2-aminonaphthalene-1,4-dione (**B(1)**) obtained are characterized through ^{1}H and ^{13}C-NMR, FTIR, mass spectrometry, single-crystal X-ray diffraction experiments, which are in conjunction with wB97X based density functional theory. Compound **A** can effectively and selectively detect Hg^{2+} and Ni^{2+} ions, and proposes a potential mechanism of action.

Keywords: Naphthoquinone; Unusual reactions; Aminonaphthoquinone; DFT; Hg^{2+} sensor.
Received: 4 January 2021; Accepted: 18 February 2021.
Article type: Research article.

1.Introduction

Currently, there has been considerable interest in molecule and ion recognition based on supramolecular chemistry. Fluorescent and colorimetric chemosensors for various analytes have been developed for physiology and medical diagnostics, particularly for heavy metal cations.[1-3] Among them, mercury being highly toxic[4] is considered to be most dangerous for human health and the environment as it can accumulate in the human body[5,6] and poses a risk for a wide variety of diseases even in minute concentrations. Mercury pollution arises through various natural activities, such as oceanic and volcanic emissions,[7,8] solid waste incineration, thermometer manufacturing, and human activities, as mercury and its derivatives are widely used in the industry. Hg^{2+} is an extremely toxic divalent metal ion and can affect many vital organs of the human body.[9] Methylmercury can be formed naturally by biomethylation of mercuric ion in the aquatic environment and is bioaccumulated in the human body through biological food chains, causing serious damage to the brain and central nervous systems.[10-13] After absorption, Hg^{2+} ions would be distributed to all biological membranes in humans and animals. It is extremely toxic because of the high affinity of mercury for thiol groups in proteins and enzymes, which leads to the dysfunction of cells and consequently results in health problems. Due to the extremely hazardous nature of mercury, numerous analytical methods have been employed to serve the purpose, such as atomic fluorescence spectrometry,[14] cold vapor atomic absorption spectrometry,[15] neutron activation analysis,[16] inductively coupled plasma mass spectrometry,[17] anodic stripping voltammetry,[18] *etc*., but all involve complex instrumentation and are time-consuming. Therefore, it becomes highly demanding to have efficient, easy-to-use chemical sensors for real-time mercury detection in environmental analyses and industrial wastewater treatments. Various colorimetric[19-21] and fluorimetric sensors[22,23] have been designed to detect the presence of the hazardous element for its elimination from the environment. Schiff'sbases,[24] benzothiazoles,[25] thiosemicarbazide,[26]

[1] *Department of Chemistry, Savitribai Phule Pune University, Pune 411007, Maharashtra State, India.*
[2] *Central Instrumentation Facility, Savitribai Phule Pune University, Pune 411007, Maharashtra State, India.*
[3] *Centre for material Characterization, National Chemical Laboratory, Pashan Road, Maharashtra State, Pune 411008, India.*
**Email:* sunita.salunke@unipune.ac.in (S. Salunke-Gawali)

lawsone,[27] anthraquinone[28] moiety and others[29] were used to develop efficient mercury sensors in solution. Many fluorescent sensors have been reported to detect mercury in an aqueous solution[30,31] at low concentrations.[32] Direct mercury detection is possible with carbon nanodots[33] and self-assembled zinc oxide nanoparticles[34] based on the mechanism of supramolecular self-assembly[35] with low detection limits.

Scientists have applied many photophysical concepts such as photo-induced electron transfer (PET),[36] resonance energy transfer[37] to enhance the efficiency of chemosensors and break the limitations.[38] Multi fluorophores systems[39] are developed by combining two or more fluorophores with different photophysical properties such as rhodamine and naphthoquinone derivatives[40] based on an energy-donor-acceptor structural design following the excitation energy transfer (ET) mechanism. When electronically connected with recognition sites, quinone derivatives are electron acceptors that have provided suitable receptors for the colorimetric sensing of various analytes. The optical characteristics[41] of the simpler quinone derivatives change on chemical transformation, and therefore they are widely used in analytical chemistry. Its absorption and fluorescence emission spectra lie within the UV (Ultraviolet) and visible regions. The various photophysical properties can be easily fine-tuned through judicious structural designs with steric and electronic features complementary to the target analytes.[42-43]

The amino group's introduction creates $\pi - \pi^*$ donor-acceptor chromophores, which absorb more intensely in the 450–500 nm region of the visible spectrum and are thus orange to red. The reaction of 2,3-dibromonaphthalene-1,4-dione with primary amines results in the formation of monosubstituted aminonaphthoquinones,[44-47] which are reported to detect various transition metal ions[48,49] as well as heavy metal ions[50] with ease.

Quinones are attracted more attention due to their numerous biological activity. Among all kinds of quinone, 2-aminonaphthoquinone moiety is an integral part of antibiotic drugs or naturally occurring quinone compounds[51] synthesized by nature under ambient conditions.[52,53] Severe conditions are necessary for their synthesis on the laboratory scale,[54] with their formation usually facilitated via several intermediates wherein the 1,4-naphthoquinone moiety serves as electrophile.[55] The reactions involving 1,4-naphthoquinones as the substrate may lead to the formation of unexpected products; few reactions are enlisted as Diels-Alder cycloaddition reaction of bis-xanthene[56]to 1,4-naphthoquinone, regioselectivity in dimerization during the synthesis of pyronaphthoquinones, ventiloquinone L[57] in the presence of cerium ammonium nitrate,[58] reactions between 5,7-dihydroxynaphthoquinone and nucleophiles[59] aryl-aryl coupling[60] in 6-bromo-1,2-naphthoquinone reactions, are some examples of unexpected reactions. On parallel lines, a remarkable regio- and -enantioselective photodimerization of naphthols in the presence of ruthenium/palladium heterometallic coordination cage via 1,4-coupling led to bi-1,2-naphthoquinone[61] as the product. Likewise, the reaction between vitamin K3 and *o*-phenylenediamine follows regioselective Michael addition yielding dihydrophenazine.[62]

In the present work, we investigate products resulting from the reactions of 2,3-dibromonaphthalene-1,4-dione and naphthalene-1,4-dione with pyridyl amines. The expected product in the reaction of 2,3-dibromonaphthalene-1,4-dione with (pyridine-2-yl)methanamine is 2-((pyridine-2-yl) methylamino)-3-bromonaphthalene-1,4-dione designated as 2MPA,[63] however, the reaction concomitantly leads to the formation of product 2-amino-3-bromonaphthalene-1,4-dione (**A**). It was further observed that the reaction of 2,3-dibromonaphthalene-1,4-dione with (pyridine-4-yl) methanamine yield the 2-aminonaphthalene-1,4-dione (**B(1)**). A similar product was obtained from the reaction of naphthalene-1,4-dione with (pyridine-2-yl)methanamine (**B(2)**). X-ray crystal structures of **A**, **B(1)**, and **B(2)** are established. The mechanism for the formation of compound **A** is presented. The density functional theory further characterized the molecular structures of **A** and **B(1)**. The vibrational frequencies, ^{1}H NMR chemical shifts, HOMO-LUMO energies are evaluated. Discernibly enough, in methanol-water solvent mixtures, compound **A** selectively detects Hg^{2+} and Ni^{2+} ions.

2. Experimental

2.1 Materials and methods

Chemicals and reagents *viz.* 2,3-dibromonaphthalene -1,4-dione(DBrNQ),naphthalene-1,4-dione, (pyridine-2-yl)metha namine, and (pyridine-4-yl)methanamine purchased from Sigma-Aldrich were used as received. Analytical grade solvents dichloromethane, chloroform, methanol obtained from Merck Chemicals. Laboratory grade toluene, methanol for chromatography were distilled by standard methods[64] and dried wherever necessary. CuCl, $CuCl_2{\cdot}2H_2O$, $NiCl_2{\cdot}6H_2O$, $ZnCl_2$, $CoCl_2{\cdot}6H_2O$ $HgCl_2$, triethylamine were obtained from Merck chemicals. $FeCl_3{\cdot}6H_2O$ procured from Qualigens Chemicals. $CrCl_3{\cdot}6H_2O$, $CdSO_4$, $MnCl_2{\cdot}4H_2O$ purchased from Fluka. $LaCl_3{\cdot}7H_2O$ was obtained from Thomas and Baker. Milli-Q water is used for the preparation of aqueous solutions.

2.2 Physical measurements

The melting point was determined using a melting point

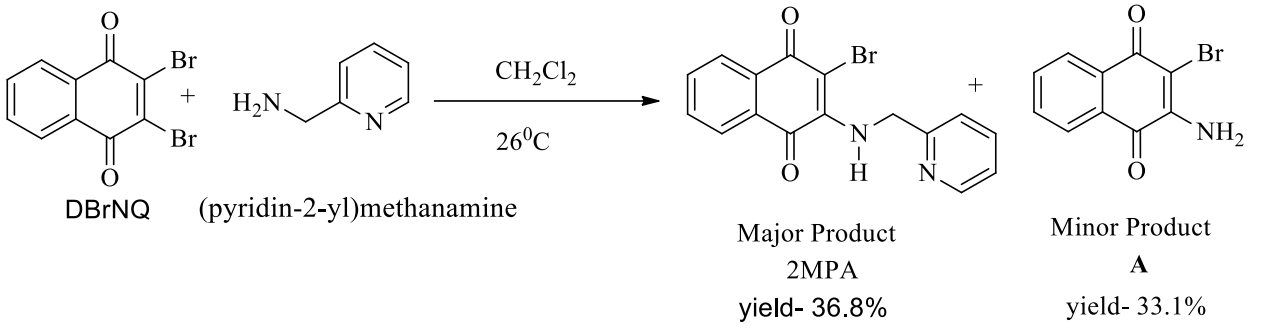

Scheme 1 Reaction scheme for the synthesis of compound **A**.

apparatus (Make-METTLER). FT-IR (Fourier-Transform Infrared) spectra recorded between 4000-400 cm^{-1} as KBr pellets on BRUKER (Tensor 37) spectrometer(Fig. S1 and Fig. S2 in ESI†).^{1}H, ^{13}C, DEPT (Distortionless Enhancement by Polarization Transfer), HSQC (Heteronuclear Single Quantum Coherence), COSY (^{1}H-^{1}H Correlation Spectroscoy) NMR (Nuclear Magnetic Resonance) recorded (Fig. S3 through Fig. S14 in ESI†) in DMSO-d_6, on Varian 500 MHz NMR instrument. TMS (tetramethylsilane) is used as a reference. The mass of compound **A** was determined by the Liquid chromatograph-mass spectrum (LC-MS) recorded on Bruker mass spectrometer (Make: IMPACT II UHR-TOF, Ultra-High Resolution Time-Of-Flight) (Fig. S15 through Fig. S17 in ESI†). The mass spectra of **A** and **B**(**1**) were also recorded on MALDI-TOF (Matrix Assisted Laser Desorption/ Ionization-Time Of Flight) (AB 4800 plus) spectrometer (Fig. S18 through Fig. S19 in ESI†). The UV-Visible spectra of **A** recorded from 200 nm to 800 nm on Shimadzu UV 1800 spectrophotometer (Fig. S20 in ESI†). Fluorescence spectra were recorded on the JASCO spectrofluorometer FP-8300 (Fig. S21 through Fig. S22 in ESI†).

2.3 Synthesis

2.3.1 Synthesis of 2-amino-3-bromonaphthalene-1,4-dione; compound A

One gram of 2,3-dibromonaphthalene-1,4-dione(DBrNQ) (3.16 mmol) was taken into a two neck round bottom flask and dissolved in 25 ml of dichloromethane (DCM) with constant magnetic stirring for about 15 min (Scheme 1) and followed by dropwise addition of the (pyridine-2-yl)methanamine (3.37 mmol, 0.330 ml). The color change of the reaction mixture has occurred from yellow to dark orange. After one hour of continuous magnetic stirring at room temperature (26 °C), the white-colored precipitate was formed, separated by decantation. The bright orange-colored solution was stirred for a further 24 hrs. The reaction was monitored by thin-layer chromatography using a 9:1 toluene and methanol solvent system. A crude product formed was isolated by evaporation of the solvent from the reaction mixture under reduced pressure.

Further, the purification carried out using column chromatography over silica gel in the methanol/toluene (1:9) system. The column chromatography indicated two separate bands, and the two products (as shown in Fig. 1) were separated. The orange fraction that eluted first corresponds to the product **A**, while the other one which comes out later was the usual Michael addition product aminonaphthoquinone ligand 2-((pyridine-2-yl)methylamino)-3-bromonaphthalene-1,4-dione. The purified orange-colored products obtained from the rotatory evaporator under reduced pressure were slowly allowed to re-evaporate at room temperature (26 ^{o}C) for 2-3 days to give beautiful bright orange-colored crystals.

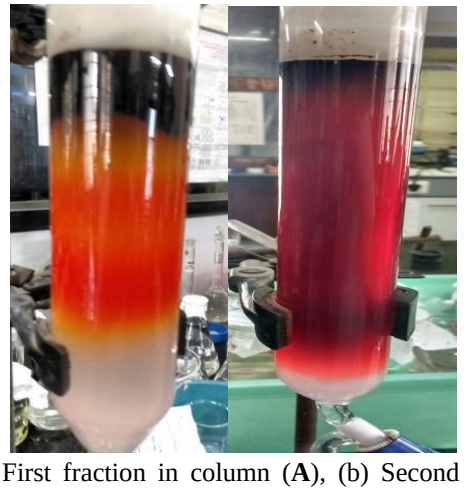

Fig. 1 (a) First fraction in column (**A**), (b) Second fraction in column (2MPA).

2.3.2 Reaction scheme for the synthesis of compound A

The yield of the pure dark orange-colored product 2MPA ligand (Fig. 1) is 0.4 g (36.8%), while that of 2-amino-3-bromonaphthalene-1,4-dione (**A**) is 0.25 g (33.1%); furthermore, if chloroform is used as a reaction solvent, only the product (**A**) is formed at room temperature (26 ^{o}C). Analytical data: Bright orange crystals. Yield: 0.25 g (33.1%). mp 190°C; FT-IR (KBr, ν_{max}/cm^{-1}): 3827, 3730, 3325, 3090, 2921, 2658, 1980, 1676, 1619, 1367, 1268, 1176, 1008, 833, 785, 720, 674, 576, 521, 450; ^{1}H NMR (499.81 MHz, $CDCl_3$) δ7.96 (d, 2H, J = 4.99 Hz,), 7.81 (t, 1H, J =7.49 Hz,), 7.73 (t, 1H, J =7.49 Hz), 7.10-7.40 (s, N-H); ^{13}C NMR ($CDCl_3$, 125.69 MHz) δ 178.75, 175.25, 148.93, 134.93, 132.73, 132.31, 129.71 126.44, 126.22, 101.42; UV-Vis (DMSO)

λ/nm)): 449; MALDI-TOF/TOF *m/z*, observed: 252.4707; $C_{10}H_6NO_2Br$ requires: 252.0711; LC-MS: *m/z* observed: 251.9, 253.8; $C_{10}H_6NO_2Br$[A] (due to isotopic bromine) requires: 252.0711.

2.3.4 Synthesis of 2-aminonaphthalene-1,4-dione; B(1), from 2,3-dibromonaphthalene-1,4-dione

0.316 g (1 mmol) of 2,3-dibromonaphthalene-1,4-dione (DBrNQ) was dissolved in 50 ml of dichloromethane (Scheme 2) and acetone (1:1, v/v) in a two neck round bottom flask and stirred for about 15 min till complete dissolution. The reactionmixture turns violet. The calculated amount of (pyridine-4-yl)methanamine (1 mmol, 0.101 ml) was added drop wise to this solution. The reaction mixture was stirred for 24 hours at room temperature (26° C) with continuous magnetic stirring until completion. The progress of the reaction was monitored on TLC (9:1 toluene and methanol solvent

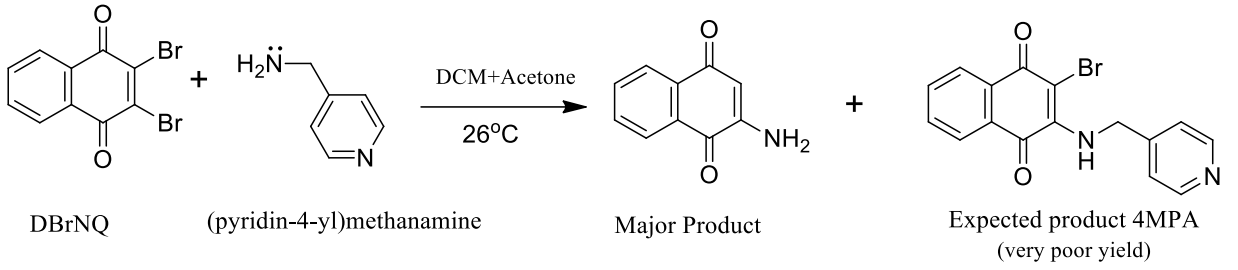

Scheme 2 Synthesis of compound **B(1)** from 2,3-dibromonaphthalene-1,4-dione.

Table 1 Illustration of crystal structure data for **A**, **B(1)** and **B(2)**.

Identification Code	**A**	**B(1)**	**B(2)**
CCDC	1504948	1446763	1510071
Empirical formula	C_{10} H_6 Br N O_2	$C_{10}H_7NO_2$	C_{10} H_7 N O_2
Formula weight	252.07	173.17	173.17
Temperature	273(2) K	296(2) K	100(2) K
Wavelength	0.71073 Å	0.71073 Å	1.54178 Å
Crystal system	Monoclinic	Monoclinic	Monoclinic
Space group	*P2₁/C*	*P2₁/C*	*P2₁/C*
Unit cell dimensions	a = 15.2305(14) Å b = 3.9184(4) Å, β = 110.700(3)° c = 15.9439(14) Å	a = 14.6144(9) Å b = 3.9568(2) Å β = 108.336(5)° c = 14.726(3) Å	a = 14.5758(6) Å b = 3.8648(2) Å β = 108.5550(10)° c = 14.6609(6) Å
Volume	890.09(15) $Å^3$	808.30(17) $Å^3$	782.96(6) $Å^3$
Z	4	4	4
Density (calculated)	1.881 Mg/m^3	1.423 Mg/m^3	1.469 Mg/m^3
Absorption coefficient	4.585 mm^{-1}	0.101 mm^{-1}	0.861 mm^{-1}
F(000)	496	360	360
Crystal size	0.24 × 0.18× 0.14 mm^3	0.319 × 0.287 × 0.241 mm^3	0.421 × 0.285 × 0.071 mm^3
Theta range for data collection	2.86 to 24.98°	2.821 to 28.439°	6.150 to 68.276°
Index ranges	-18<=h<=18, -4<=k<=4, -18<=l<=14	-19<=h<=19, -5<=k<=5, -19<=l<=19	-17<=h<=17, -4<=k<=4, -17<=l<=17
Reflections collected	5752	14289	4266
Independent reflections	1532 [R(int) = 0.0861]	2020 [R(int) = 0.1340]	1341 [R(int) = 0.0254]
Completeness to theta = 24.98°	97.1 %	99.9%	93.4 %
Absorption correction	Semi-empirical from equivalents	Semi-empirical from equivalents	Semi-empirical from equivalents
Max. and min. transmission	0.5661 and 0.4058	-	0.941 and 0.745
Refinement method	Full-matrix least-squares on F^2	Full-matrix least-squares on F^2	Full-matrix least-squares on F^2
Data / restraints / parameters	1532 / 0 / 127	2020 / 0 / 119	1341 / 0 / 118
Goodness-of-fit on F^2	1.122	1.003	1.042
Final R indices [I>2sigma(I)]	R1 = 0.0617, wR_2 = 0.1515	R_1 = 0.0726, wR_2 = 0.1125	R1 = 0.0381, wR_2 = 0.1017
R indices (all data)	R1 = 0.0853, wR_2 = 0.1635	R1 = 0.1853, wR_2 = 0.1443	R1 = 0.0410, wR_2 = 0.1046
Largest diff. peak and hole	0.688 and -0.465 e.$Å^{-3}$	0.195 and -0.193 e.$Å^{-3}$	0.174 and -0.233 e.$Å^{-3}$

system). The crude product was filtered and purified by column chromatography over silica gel in the methanol/toluene (1:9) system. It showed a separate orange band on the column apart from the violet band. The orange fraction that eluted first corresponds to the unexpected product. The purified orange-colored solid product obtained from rotary evaporator under reduced pressure was slowly allowed to re-evaporate at room temperature (26 °C) for 2-3 days in toluene-methanol eluent to give beautiful dark orange-colored crystals. The crystal data obtained is represented as **B(1)** in Table 1.

We attempted this reaction under various reaction conditions, such as in

i) in DCM,
ii) DCM in the presence of base triethylamine,
iii) in DCM and sodium acetate,
iv) in DCM and methanol,
v) in ethanol, both the base's absence/presence at room temperature (26 ^{o}C) and under refluxed conditions, but no noticeable results were obtained. The yield of the expected aminonaphthoquinone was feeble.

2.3.5 Analytical Data of 2-aminonaphthalene-1,4-dione; B(1)

Dark orange crystals. Yield: 0.188 g (79%); FT-IR (KBr, ν_{max}/cm^{-1}): 3381, 3066, 2995, 2918, 2686, 2486, 1961, 1865, 1681, 1620, 1564, 1421, 1359, 1269, 1219, 1124, 985, 889, 825, 781, 723, 663, 594, 532, 491; ^{1}H NMR ($CDCl_3$, 499.84 MHz)δ 8.16 (d, *J* = 6.99 Hz, 1H, Ar), 8.07 (d, *J* = 7.99 Hz, 1H), 7.73 (m, *J* = 7.75 Hz, 1H), 7.66 (m, *J* = 7.49 Hz, 1H), 7.27 (s, 1H). (5.0-6.35 Hz, 2H, NH_2); ^{13}C NMR ($CDCl_3$, 125.70 MHz) δ 178.50, 176.31, 147.16, 134.89, 132.64, 129.69, 127.23, 126.74, 105.15, 77.02; MALDI-TOF: *m/z* observed 172.2298, $C_{10}H_6NO_2$ requires 172.1621.

2.3.6 Synthesis of 2-aminonaphthalene-1,4-dione; B(2), from naphthalene-1,4-dione

One mmol of naphthalene-1,4-dione (0.2 g) dissolved in 20 ml dry methanol, and the mixture stirred for about 15 min. One mmol of (pyridine-2-yl)methanamine (~0.10 ml) was added dropwise to this solution. The color of the solution changes from yellow to orange-red. The reaction mixture was stirred for 24 hours at room temperature (26 °C) with constant magnetic stirring. The formation of the product was monitored by TLC (methanol/toluene 1:9). Dark red-colored solid was obtained by evaporation and further purified by column chromatography using silica as the stationary phase and toluene: methanol (9:1) as eluent. After evaporation, dark red-colored crystals were obtained. Yield: 0.121 g (65.76%). The crystal data obtained represented in Table 1 as **B(2)**. There is also the formation of 2-((pyridine-2-yl)methylamino)naphthalene-1,4-dione observe d for this reaction; however, when the synthesis carried out in toluene, only compound **B(2)** resulted as a final major product.

2.4 Single crystal X-ray diffraction

Single crystal X-ray diffraction data for **A**, **B(1)** and **B(2)** were collected on D8 Venture PHOTON 100 CMOS diffractometer using graphite monochromatized Mo-K_α radiation (λ = 0.7107 Å) with exposure /frame = 10 secs. The X-ray generator operated at 50 kV and 30 mA for Mo-K_α radiation with 50 kV and one mA for Cu-K_α. An initial set of cell constants and an orientation matrix were calculated from 24 frames and 60 frames for Mo and Cu sources. The optimized strategy used for data collection consisted of different φ and ω scans with 0.5° steps in φ/ω. Crystal to detector distance was 5.00 cm with 512 × 512 pixels/frame, Oscillation/frame -0.5º, maximum detector swing angle = -30.0º, beam centre = (260.2, 252.5), in-plane spot width = 1.24. Data integration was carried out with a Bruker SAINT program, and empirical absorption correction for intensity data carried out subsequently by Bruker SADABS. The programs are integrated into the APEX II package.[65] The data corrected for Lorentz and polarization effect. The structures were solved by *Direct Method* using SHELX-97.[66] The final refinement of the structure was performed by full-matrix least-squares techniques with anisotropic thermal data for non-hydrogen atoms on F2. The non-hydrogen atoms were refined anisotropically, while hydrogen atoms were refined at the calculated positions as riding atoms with isotropic displacement parameters. Molecular diagrams generated using Mercury program.[67] Geometrical calculations were performed using SHELXTL[66] and PLATON.[68]

2.5 Computational details

Compounds **A** and **B(1)** were optimized, employing the ωB97X based density functional theory[69]using the Gaussian-09 program.[70] The internally stored 6-31G basis set with diffuse functions added to the basis of heavier atoms (denoted by 6-31+G(d,p) basis) was used.[71] The stationary point structure was confirmed to be the local minimum on the potential energy surface through vibrational frequency computations. Frontier orbitals are derived within the same framework of the theory. Time-dependent Density Functional Theory (TD-DFT) computations predict wavelength maxima in **A** and **B(1)**.

2.6 Metal ion binding studies of A

Metal ion binding studies were studied[44-47] by following methods, (i) in dry methanol solution of chemosensor **A** and metal ions (1×10^{-4} M); (ii) 1×10^{-4} M solution of (i) in the presence of triethylamine; (iii) methanol (chemosensor (1×10^{-4} M) and water (metal ion, 1×10^{-4} M) mixture; and (iv) 1×10^{-4} M solution of (iii) in the presence of triethylamine. In all methods, 2 ml of chemosensor, *i.e.*, compound **A** (1×10^{-4} M), mixed with 2 ml of metal ion solution at room temperature (26 °C). 1 ml triethylamine added to

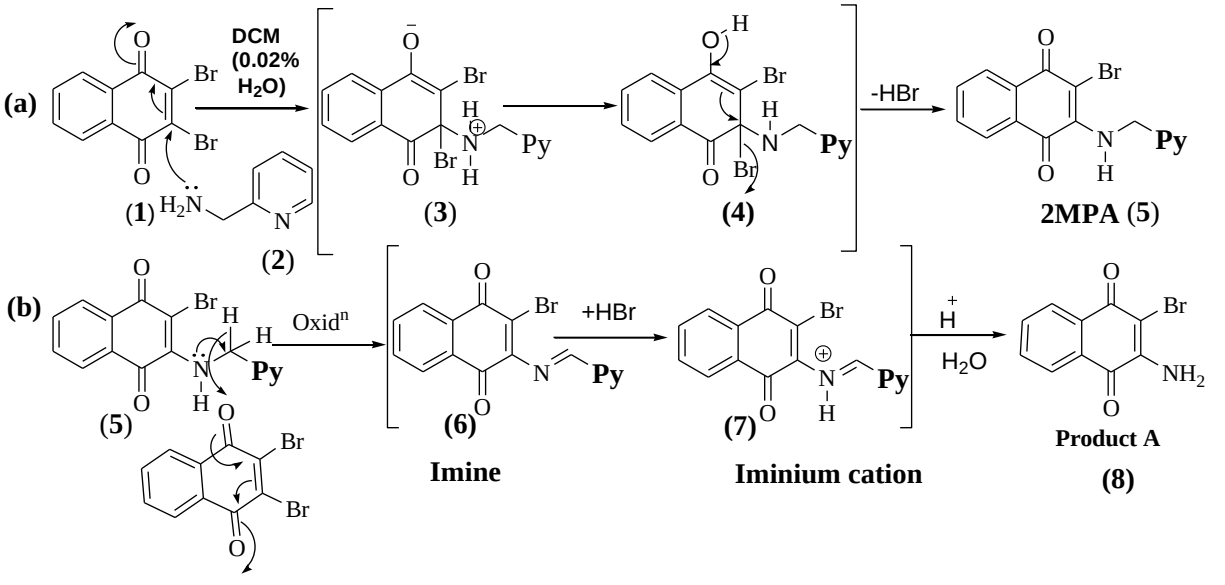

Scheme 3 Plausible reaction mechanism involved in the synthesis of a) 2MPA and b) Unusual Product **A**.

chemosensor solution in case of (ii) and (iv)before the addition of metal ion solution. UV- visible and fluorescence spectra of all the solutions were measured after mixing the ligand and metal ion solution with a concentration of 1×10^{-4} M each.

3. Results and Discussion

3.1 Reaction mechanisms accompanying synthesis of 2-amino-3-bromonaphthalene-1,4-dione; A

Formation of product **A** observed in the synthesis of 2MPA. Product **A** was isolated and characterized as 2-amino-3-bromonaphthalene-1,4-dione. This product is characterized by FT-IR, ^{1}H, ^{13}C-NMR, gDQCOSY (Gradient double Quantum Filtered Correlation Spectroscopy), DEPT experiments.

The plausible mechanism for the formation of product **A** is shown in Scheme 3. Herein, Michael's addition of the 2,3-dibromonaphthalene-1,4-dione (DBrNQ)(**1**) reacts with (pyridine-2-yl)methanamine (**2**) in DCM (0.02% water) used as a solvent resulting in the formation of 2MPA (**5**) via in situ generation of the anion (**3**), followed by proton shifting and loss of –HBr molecule from (**4**). After the formation of 2MPA(**5**) was oxidized in the presence of an excess of DBrNQ (**1**), resulting in corresponding imine (**6**), which leads to intermediate iminium cation formation (**7**) by nucleophilic attack of the bromide anion present in the solution and then further hydrolysis to form compound (**8**) in the final step. It was isolated and fully characterized by FT-IR, ^{1}H- and ^{13}C-NMR spectroscopic techniques. Finally, the structure of the product **A** confirmed by Single Crystal X-ray diffraction studies.

The product 2-aminonaphthalene-1,4-dione **B(1)** is obtained from the reaction of 2,3-dibromonaphthalene-1,4-dione and (pyridine-4-yl)methanamine. A similar product was obtained from the reaction of naphthalene-1,4-dione and (pyridine-2-yl) methanamine; it is designated as **B(2)**. Plausible reaction mechanism of compound **B(1)** presented in Scheme S1 and Scheme S2 (in ESI†).

3.2 FT-IR and NMR Studies

The FT-IR spectrum of compound **A** (**8**) shows the characteristic band at 1676 cm^{-1} and 1619 cm^{-1}, assigned to$\nu_{C=O}$ vibrations of naphthalene-1,4-dione. The other distinctive bands that appear at 3350 and 3461 cm^{-1}, respectively (Fig. S1 in ESI†) are due to the presence of ν_{N-H} stretching of the amino functionality of product **A** (8). Further, the FT-IR band at 674 cm^{-1} corresponds to ν_{C-Br} stretching, which gives a fair idea about the bromine's retention in compound '**A**'.[63] The ν_{N-H} stretching frequency was found near 3379 cm^{-1} (Fig. S2 in ESI†) for **B(1)** while $\nu_{C=O}$ vibrations here was located near1654 and 1634 cm^{-1}

^{1}H NMR spectrum of the unique product **A**, recorded in $CDCl_3$ solvent (Fig. S3 in ESI†), reveals two multiplets in the aromatic region δ = 7.73-8.00 ppm, indicating the presence of four protons of naphthoquinone moiety. While the other proton signals at ~δ = 7.10-7.40 ppm results from the NH_2 group of **A**.

^{13}C NMR spectrum of A shows signals at δ = 175.25 ppm and δ = 178.75 ppm (Fig. S4 in ESI†) for two carbonyl groups naphthalene-1,4-dione moiety. Four quaternary carbons are thus evident. The ^{13}C chemical shift signals appearing at δ = 132.30 ppm and δ = 129.70 ppm correspond to the ring junction of phenyl functionality fused with quinone. The remaining two quaternary carbon signals indicate Br by NH_2 group's substitution with C-NH_2 being downfield to 148.93 ppm. The signal appearing at 126.21 ppm is due to the C-Br bond of the starting material DBrNQ.

^{1}H and ^{13}C NMR spectra of **B**(**1**) recorded in the $CDCl_3$ solvent are shown in Fig. S7 and Fig. S8 of ESI†. Besides, gHSQCAD and gDQCOSY are displayed in Figs. S9 and S10

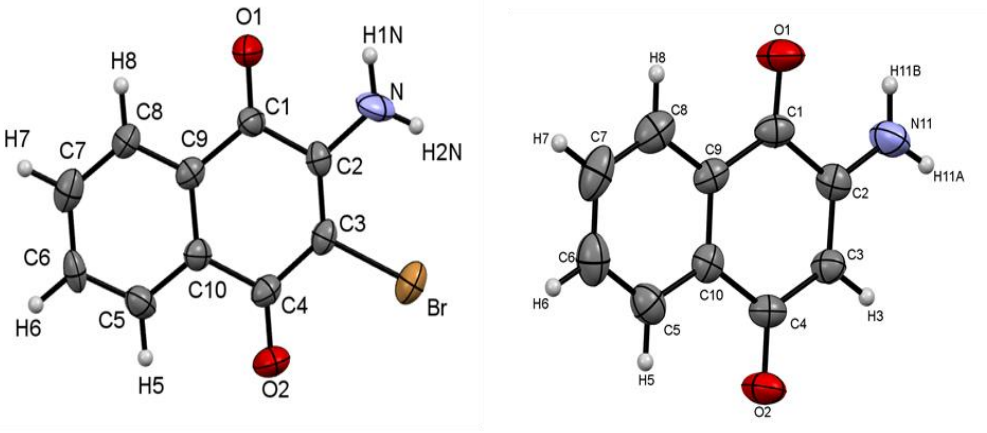

Fig. 2 ORTEP of compound **A** (left) and **B(1)** (right), the ellipsoids are drawn with a 50% probability.

of the ESI†. The ^{1}H NMR spectrum **B(1)** reveals two multiplets in the range 7.66-8.16 ppm, integrating four hydrogens of the α-naphthoquinone moiety in the desired compound. NH_2 substituent moves to absorb between δ = 5.0-6.35 ppm, whereas the C-3) proton adjacent to the amino group absorbs at δ = 7.27 ppm.

Two signals at δ = 176.31 ppm and δ = 178.50 ppm on the ^{13}C NMR spectrum are characteristic of the two carbonyl groups on naphthalene-1,4-dione moiety. The ^{13}C NMR signals, which reveal the most about the substitution pattern of these compounds, arise at δ = 147.158 ppm (C-2) and δ = 105.151 ppm (C-3) (Fig. S5 in ESI†).

The molecular mass of compound **A** has been determined by different mass spectral techniques such as LC-MS and MALDI-TOF experiments (Fig. S16 and Fig. S19in ESI†). For compound **A**, the mass was found to be 252.4707 m/z.

3.3 Single Crystal X-ray diffraction

Compounds **A** and **B(1)** crystallize in monoclinic space group *P2₁/C*. ORTEP diagrams of compound **A** and **B(1)** are shown in Fig. 2, and the crystal structure data presented in Table 1. The hydrogen bond parameters are summarized in Table 2 (bond distances in Table S2, Table S7 of, and Table S11 in ESI†). The carbonyl bond distances (~1.21Å and ~1.23Å) compared well with those in its oxidized form reported earlier.[72-77]

As can be noticed, compound **A** is associated with neighboring five molecules via N-H···O, N-H···Br, and Br···O interactions (Fig. 3). Each molecule is associated as a dimer unit, which facilitates intermolecular N-H···O interaction and is linked via Br···O Fig. 4a. A butterfly-like arrangement extending down the c-axis is displayed in Fig. 4b.

Table 2 Hydrogen bonding geometries and other molecular interactions for **A** and **B(1)**.

	D-H···A	D-H(Å)	H···A(Å)	D···A(Å)	∠D-H···A(°)	Symmetry
A	N-H(1N)···O(1)	0.880	2.446	2.744(9)	100.4	Intra
	N-H(1N)···O(1)	0.880	2.261	3.02(1)	144.3	1-x,-y,2-z
	N-H(2N)···Br	0.880	3.173(7)	3.7061)	133.6	1-x,-1/2+y,2.5-z
	Br(1)···O(1)	-	-	3.173	-	x,-1/2-y,-1/2+z
B(1)	N(11)-H(11B)···O(1)	0.860	2.350	2.680(3)	103.1	Intra
	N(11)-H(11B)···O(2)	0.860	2.190	2.919(3)	142.3	-x,-1/2+y,1/2-z
	N(11)-H(11B)···O(2)	0.860	2.216	3.042(3)	160.9	x,1.5-y,-1/2+z
	C(5)-H(5)···O(1)	0.929	2.642	3.363(4)	135.0	x,1/2-y-1/2+z

Table 3 Selected bond distances (in Å) in **A** and **B(1)** in the gas phase (G) and dimethylsulfoxide (D).

	A(Å)		Observed (Å)	**B(1)**(Å)		Observed(Å)
	G(Å)	D(Å)		G(Å)	D(Å)	
C(4) = O(2)	1.218	1.217	1.217	1.224	1.224	1.240
C1=O1	1.219	1.217	1.217	1.219	1.219	1.216
C- N	1.344	1.344	1.430	1.351	1.351	1.331
C-Br/C-H	1.872	1.872	1.885	1.086	1.086	0.930

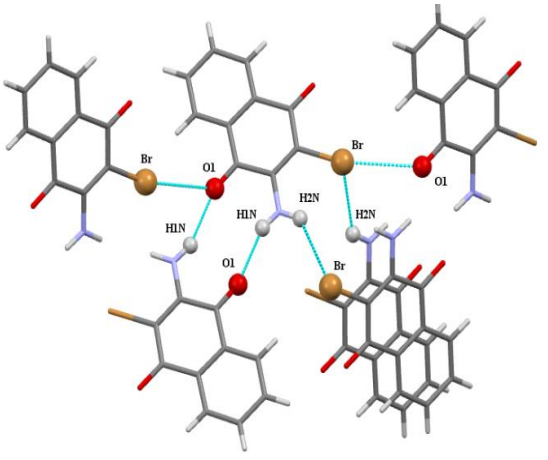

Fig. 3 Molecular association of **A** with neighboring molecules.

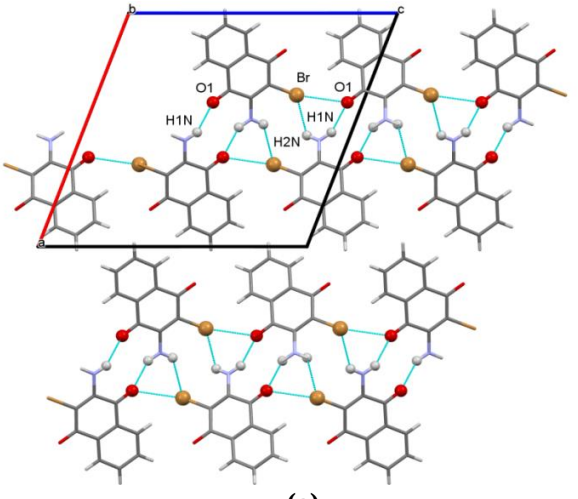

(a)

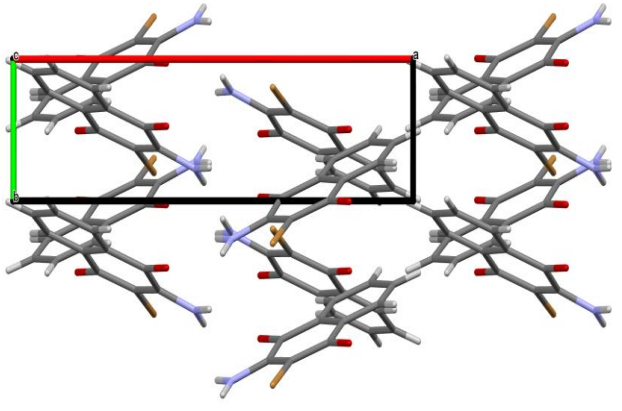

(b)

Fig. 4 Molecular packing in **A** down the a) b-axis and b) c-axis.

Molecule B(1) shows intra and intermolecular N-H···O hydrogen bonding interaction. Six other similar molecules surround each molecule of **B(1)** via C-H···O, N-H···O, and C-H···π interactions (Fig. 5). Tetrameric molecular unit of **B(1)** molecules (Fig. 6) formed by N-H···O (N(11)-H(11A)···O(2); -x,1/2+y, +1/2-z and N(11)-H(11B)···O(2); x, 1.5-y, +1/2+z) interaction and also supported by C(3)-H(3)···π (3.57 Å, -x,1/2+y, 1/2-z) interaction (Fig. 6).

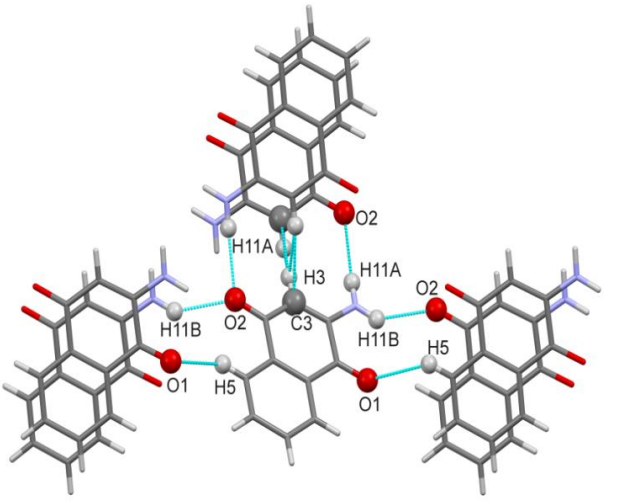

Fig. 5 Molecular association of **B(1)**.

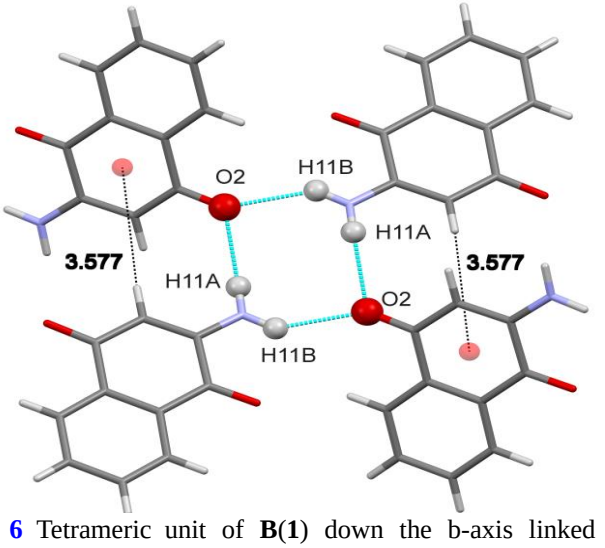

Fig. 6 Tetrameric unit of **B(1)** down the b-axis linked via N-H···O interactions.

3.4 DFT investigations

Optimized structures of naphthoquinone derivatives **A** and **B(1)** from the ωB97X based DFT are depicted in Fig. 7. The observed and calculated bond distances and bond angles are shown in Table 3. The carbonyl C(1)-O(1) bond distances became 1.219 Å in **A**. The longer corresponding bond in **B(1)** compared to **A** attributed to intramolecular N-H···O hydrogen bonding. ^{1}H NMR chemical shifts (δ_H) in **A** and **B(1)** in DMSO (as solvent) simulated through the SCRF-PCM (Self Consistent Reaction Field- Polarizable Continuum Model) theory. A comparison with the measured spectra presented in Table 4. As shown, H1A proton participating in N-H···O interactions in **B(1)** emerge with relatively large deshielding (5.7 ppm) relative to the H1B proton in the spectrum. Aromatic proton signals show up in the 8.3 to 9.0 ppm region.

Structural ramifications to vibrational spectra can be noticed in Table 5. Theoretical vibrational frequencies (harmonic) reported were scaled by a factor of 0.91. As may be seen, the C(1)O(1) carbonyl stretching in **A** assigned to

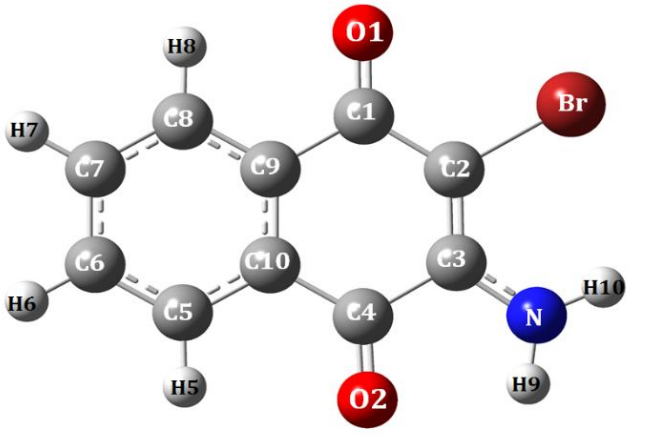

(a)

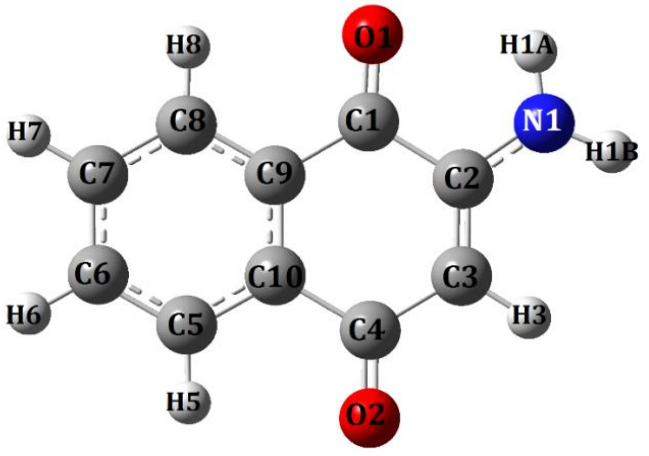

(b)

Fig. 7 Optimized structures of **A** and **B(1)**.

Table 4 ^{1}H chemical shift (in ppm) in dimethylsulfoxide.

	A	Observed	**B(1)**	Observed
H(1A)	-		5.7	-
H(1B)	-		4.8	5.0-6.35
H(3)	-		6.2	7.27
H(5)	8.7	8.15	8.8	8.16
H(6)	8.2	7.71	8.4	7.72
H(7)	8.3	7.71	8.3	7.76
H(8)	8.7	8.15	9.0	8.06
H(9)	6.1	2.19	-	-
H(10)	5.0			

the 1639 cm^{-1} (Fig. 8) vibration that corresponds to the 1628. cm^{-1} vibration in **B(1)**. The aromatic stretching was predicted at ~2962 cm^{-1} (Fig. 9). These inferences agree well with the experiment. Frontier orbitals HOMO and LUMO (isosurface of ±0.04 au) in the aminonaphthquinones are portrayed (Fig. 10 and Fig. 11). HOMO of both derivatives extended over the entire molecule and rendered with a large π-character, whereas the LUMO reveals significant σ-character. Electronic spectra of these were computed in the presence of methanol using the TD-DFT theory.

Table 5 Selected vibrational frequencies (in cm^{-1}, ν) of **A** and **B(1)**.

Vibrations	**A**	Observed	**B(1)**	Observed
ν(CH)	2964	2922,	2852	2961
ν(C1=O1)	1639	1614	1628	1634
ν(C4=O2)	1656	1676	1654	1654
ν(C=C)	1564	1572	1571	1578
ν(NH_2)	3441	3459	3457	3379
	3317	3348	3322	3298

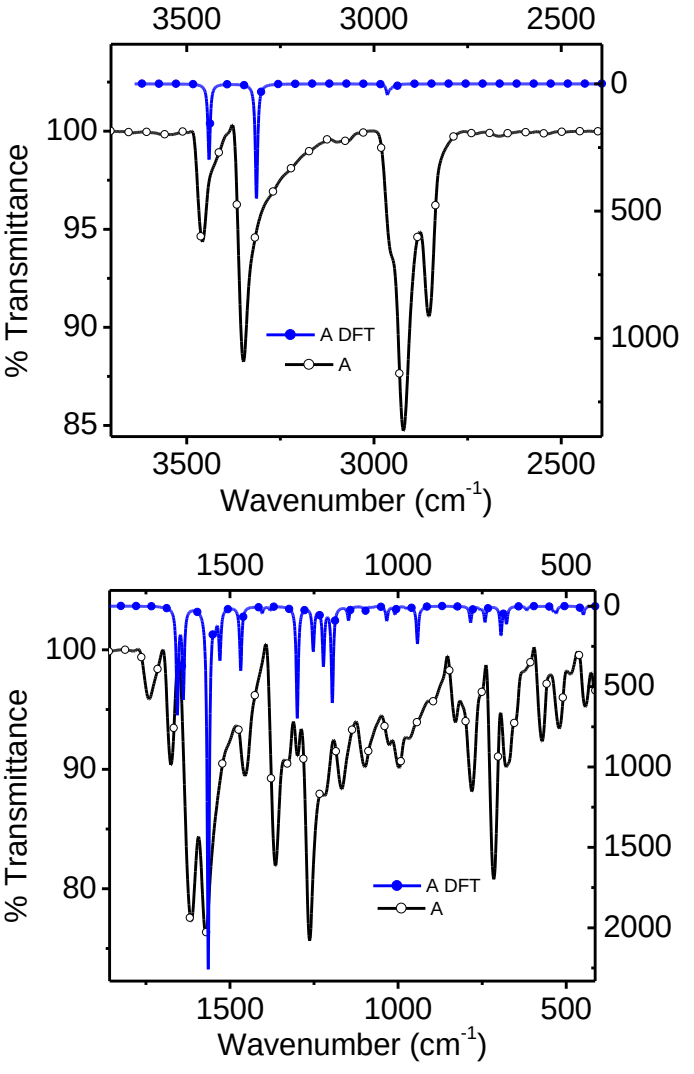

Fig. 8 Experimental and calculated FT-IR spectrum of **A**.

The wavelength maxima, oscillator strengths, and orbital descriptors have been summarized in Table 6. As is transparent, the absorption band arising from the HOMO to LUMO transition shows up near ~382 nm and 373 nm for **A** and **B(1)**, respectively. The HOMO-LUMO energies, global indices of reactivity *viz.*, chemical potential (μ), hardness (η),

electrophilicity (ω) of amino naphthoquinone derivative, and its anionic form summarized in Table 7. A separation of HOMO and LUMO energies (ΔE) in the molecule implies the reluctance toward accepting electrons in the LUMO and removing an electron from the HOMO, which explains why **A** is more stable.

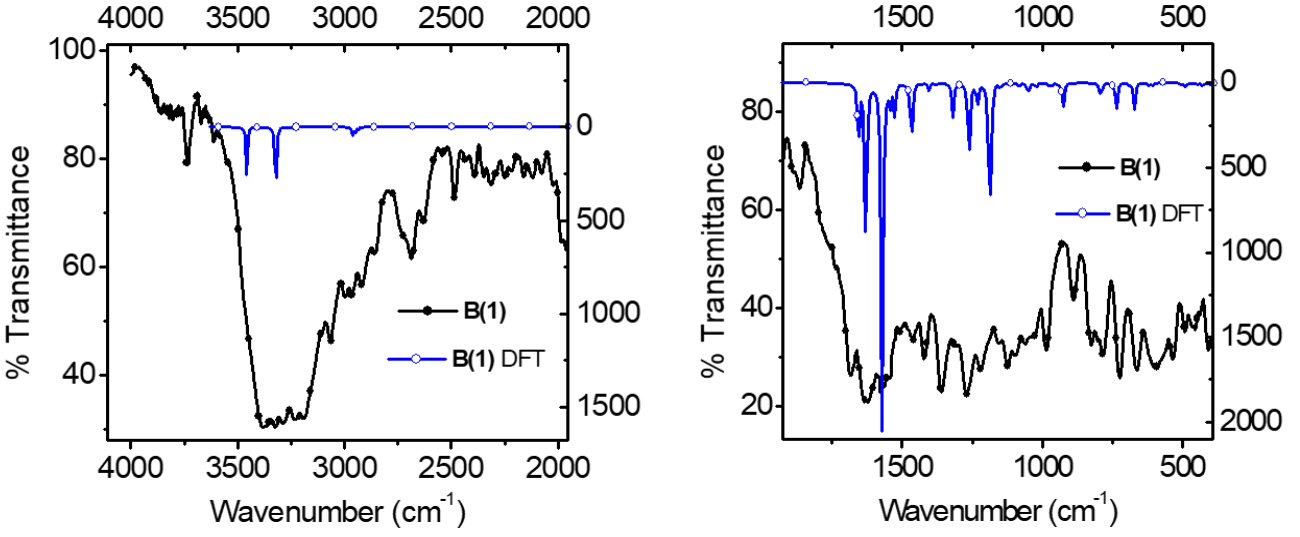

Fig. 9 Experimental and Calculated FT-IR spectrum of **B(1)**.

Table 6 Separation of HOMO, LUMO energies, and global indices in **A** and **B**(1).

	A			**B(1)**		
Transition	E_{ex}	λ_{max}	(*f*)	E_{ex}	λ_{max}	(*f*)
HOMO → LUMO	3.2	382	0.067	3.3	373	0.015
HOMO → LUMO +1	5.7	218	0.535	5.7	216	0.510
HOMO → LUMO +2	6.4	194	0.020	6.5	191	0.374
HOMO → LUMO +3	6.5	190	0.332			
HOMO -1→ LUMO	4.4	280	0.112	4.5	277	0.098
HOMO -1 → LUMO +1	4.9	256	0.355	6.3	197	0.079
HOMO -1 → LUMO +2				7.4	168	0.380
HOMO -2 → LUMO	3.2	382	3.2	4.9	254	0.372
HOMO -2 → LUMO +1	4.4	280	4.4	6.2	199	0.045
HOMO -4 → LUMO	6.5	190	6.5	4.8	259	0.302

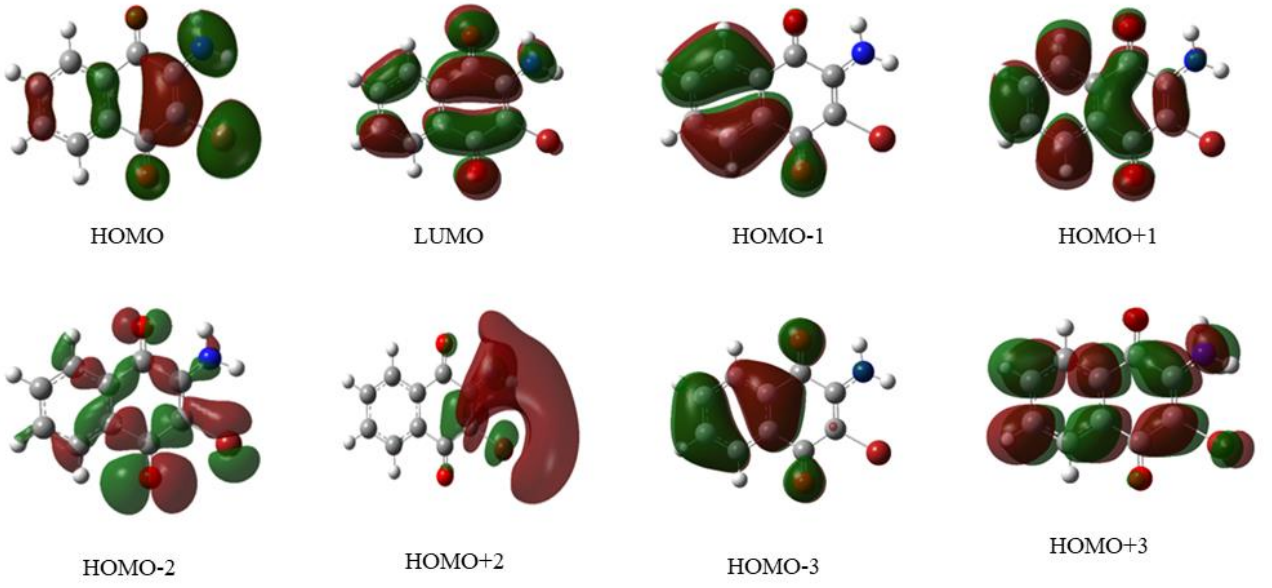

Fig. 10 Representative frontier orbital's in **A.**

Table 7 Wavelength maxima (λ_{max}(nm), oscillator strengths (f),and assignments of bands in the electronic spectra of the monomer **A** and **B(1)** in methanol from TDDFT.

Molecular properties	A	B(1)
ΔE HOMO-LUMO	0.278	0.293
Softness(σ)	7.202	6.824
Global hardness (ŋ)	0.139	0.147
Electronic chemical potential (μ)	-0.186	-0.186
Electronegativity(χ)	0.186	0.186
Global electrophilicity index (ω)	0.125	0.017

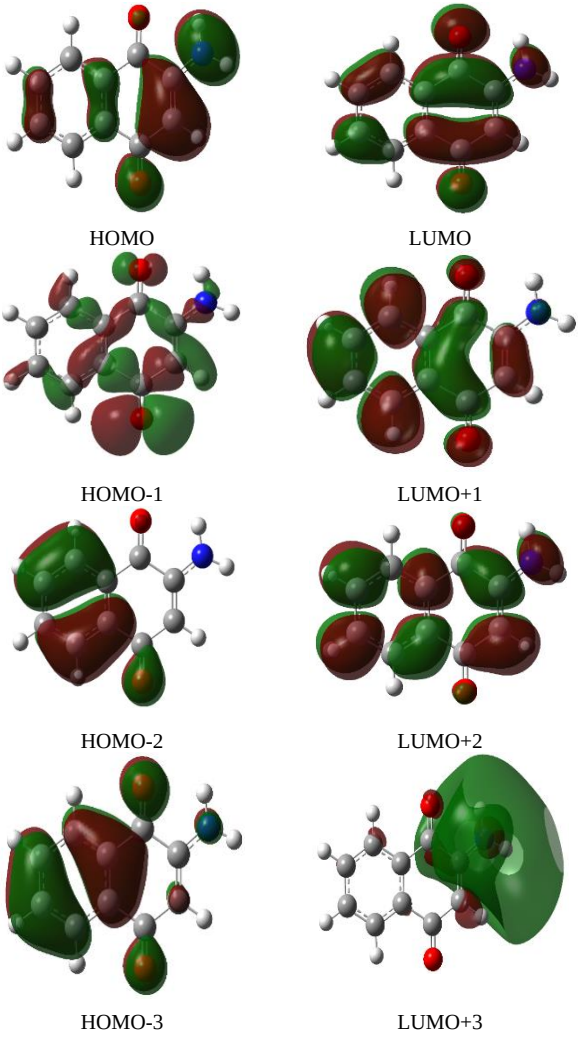

Fig. 11 Most representative frontier orbital's **B(1)**.

3.5 Chemosensor ability of compound A

Molecular recognition of fluorescent and colorimetric chemosensors of various analytes with potential applications in physiology and medical diagnostics, particularly the heavy metal cations,[1-3] has been the focus of attention within the domain of supramolecular chemistry. Amongst these, in particular, mercury with high toxicity[4] and its trace amounts, causing adverse effects to human health,[5-8] has been of considerable interest in the literature.[5,6]

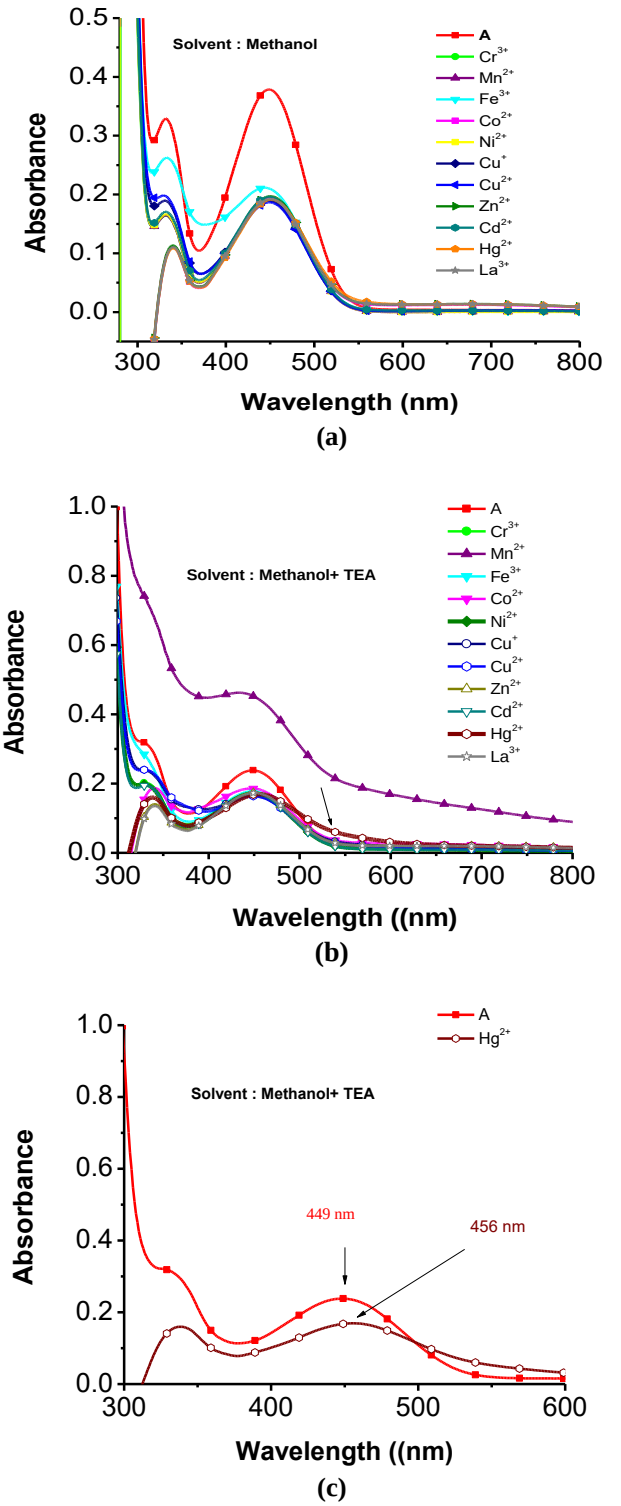

Fig. 12 A UV-visible spectrum of **A** (10^{-4} M) methanol in the presence of transition metal ions (a) in methanol, (b) UV-visible spectra of **A** (10^{-4} M) in methanol and triethylamine in the presence of transition metal ions (c) UV-visible spectra of **A** and Hg^{2+} solution.

The metal binding ability of compound **A**, evaluated with various metal ions (Cr^{3+}, Mn^{2+}, Fe^{3+}, Co^{2+}, Ni^{2+}, Cu^{2+}, Zn^{2+}, Hg^{2+}, La^{3+}, and Cd^{2+} spectrophotometrically and fluorescence measurements in different solvents including i)

pure dry methanol (Fig. 12), ii) methanol and water mixture (1:1) (v/v) of the ligand in methanol and metal ion solutions in Millipore water, iii) in the presence of a mild base like triethylamine (TEA) in methanol and methanol-water mixture as well (Fig. S20 in ESI†). As observed, compound **A** shows color change, specifically only with a few metal ions.

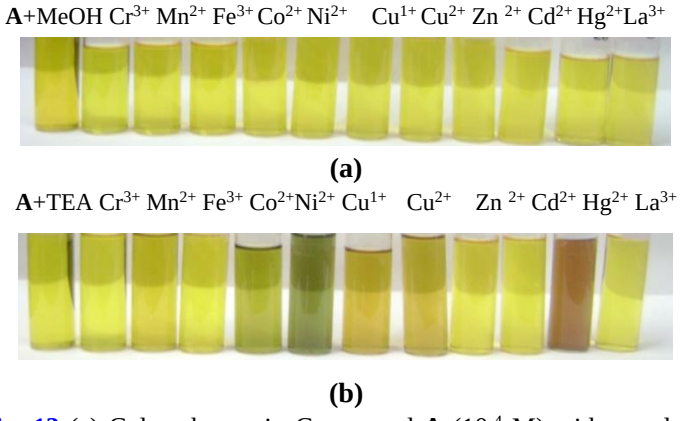

Fig. 13 (a) Color change in Compound **A** (10^{-4} M) with metal ions (10^{-4} M) in methanol (b) Compound **A** (10^{-4} M) with metal ions (10^{-4} M) in methanol and triethylamine.

Furthermore, a highly selective colorimetric response towards mercuric ions can be easily detected by the naked eye in the presence of base triethylamine in the methanol system. Its solution reveals an instant change in color from greenish-yellow to brick red (Fig. 13), that accompanies the metal complex formation. Moreover, compound **A** did not respond to the metal ion in the methanol/water system with or without the base triethylamine. The UV-visible spectrum of the ligand was nearly insensitive to the presence of a solvent. Compound **A** revealed the absorption maximum at 449 nm in methanol with and without base and likewise methanol-water mixture with TEA or without TEA as well (Fig. S20 in ESI†). Photographs in the methanol system are shown in Fig. 14. This figure shows that the yellow color of ligand (compound **A**) was changed to brown on addition of Hg^{2+} and greenish with on Ni^{2+}, respectively.

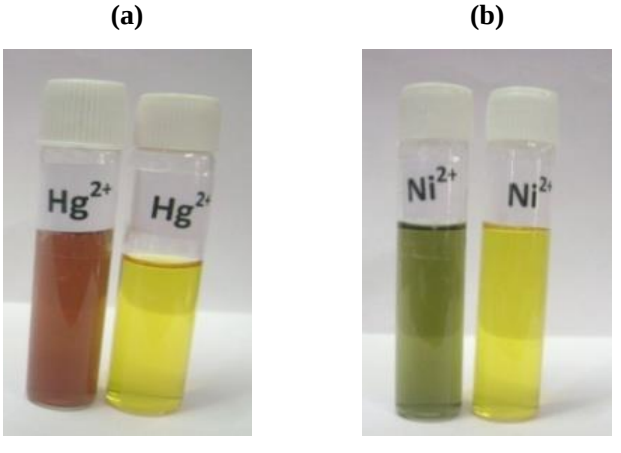

Fig. 14 Change in mercury color in solution in the presence of a base and the absence of a base for Hg^{2+} and Ni^{2+}.

The fluorescence behavior of ligands was assessed in different solvents. Spectra were recorded at 450 nm and 350 nm, shown in Fig. S21 and Fig. S22 of ESI†. As may readily be observed, the compound solution shows enhanced fluorescence intensity toward Zn^{2+} ions in the presence of triethylamine.

4. Conclusions

The products of the reaction of 2,3-dibromonaphthalene-1,4-dione with (pyridine-2-yl)methanamine (**A**) and (pyridine-4-yl)methanamine (**B(1)**) have been reported. A mechanism of the formation of **A** (2-amino-3-bromonaphthalene-1,4-dione) and **B(1)** (2-aminonaphthalene-1,4-dione) is proposed. The compounds were characterized using FT-IR, NMR, mass spectroscopy, and single-crystal X-ray diffraction studies. X-ray structure reveals that compound **A** is associated with the five, whereas the compound **B(1)** to six nearest similar molecules via N-H···O and the Br···O interactions. Besides the compound **A** also shows N-H···Br interaction. The inferences on structure and spectra are corroborated through the density functional theory. It has been demonstrated that compound **A** remarkable exhibit selectivity towards Hg^{2+} and Ni^{2+}ions in methanol in the presence of a mild base, which is accompanied by a color change from greenish-yellow to brick red.

Supplementary Information

†Electronic Supplementary Information (ESI).
FT-IR figures Fig.S1 to Fig.S2, NMR Figures Fig.S3 through Fig. S14, LC-MS Fig.S15 to Fig.S17, MALDI-TOF Fig. S18 and Fig.S19. Crystallography Table S1 through Table S14. CambridgeCrystallographic Data Centre and may be obtained on request quoting the deposition number CCDC numbers 1504948 for **A**, 1446763 for **B(1)**, and 1510071 for **B(2)** from the CCDC, 12 Union Road, Cambridge CB21EZ, UK (fax: +44 1223 336 033; E-mail address: deposit@ccdc.cam.ac.uk).

Acknowledgments

SSG is grateful to DST-SERB(Ref. No. EMR/2016/007912). SPG acknowledges support from the Research Project (37(2)/14/11/2015-BRNS) from the Board of Research in Nuclear Sciences (BRNS), India. DNL grateful to New Delhi, India, for the Senior Research Fellowship and Savitribai Phule Pune University for the award of research fellowship through the University of Potential excellence scheme from the University Grants Commission, New Delhi, India. SPG thanks the Centre for Development of Advanced Computing (C-DAC), Pune, for computer time at the National Param Supercomputing Facility.

Supporting information

Applicable

Conflict of interest

There are no conflicts to declare.

References

[1] H. Wang, L. Xue, C. Yu, Y. Qian and H. Jiang, *Dyes Pigm.*, 2011, 350-355, doi:10.1016/j.dyepig.2011.04.007.

[2] A. Pal and B. Bag, *J Photochem. Photobio. A.*, 2012, **240**, 42-49, doi:10.1016/j.jphotochem.2012.05.010.

[3] R.T. Bronson, D.J. Michaelis, R.D. Lamb, G.A. Husseini, P.B. Farnsworth, M.R. Inford, R.M. Izatt, J.S. Bradshaw and P.B. Savage, *Org. Lett.*, 2005, **7**, 1105-1108, doi: 10.1021/ol050027t.

[4] X.B. Zhang, C.C. Guo, Z.Z. Li, G.L. Shen and R.Q. Yu, *Anal. Chem.*, 2002, **74**, 821-825, doi: 10.1021/ac0109218.

[5] S.D. Richardson and T.A. Temes, *Anal. Chem.*, 2005, **77**, 3807-3838, doi: 10.1021/ac058022x.

[6] X. Zhang, Y. Xiao and X. Qian, *Angew. Chem. Int. Ed.*, 2008, **47**, 8025-8029, doi: 10.1002/anie.200803246.

[7] A. Renzoni, F. Zino and E. Franchi, *Environ. Res.*, 1998, **77**, 68-72, doi: 10.1006/enrs.1998.3832.

[8] J.M. Benoit, W.F. Fitzgerald and A.W. Damman, *Environ. Res* , 1998, **78,** 118-133, doi: 10.1006/enrs.1998.3850.

[9] T.A. Baughman, *Environ. Health Perspect.*, 2006, **114**, 147–152. doi:10.1289/ehp.7048.

[10] M. Harada, *Crit. Rev. Toxicol.*, 1995, **25**, 1-24, doi: 10.3109/10408449509089885.

[11] I.A. Onyido, R. Norris and E. Buncel, *Chem. Rev.*, 2004, **104**, 5911-5930, doi:10.1021/cr030443w.

[12] J.S. Lee, M.S. Han and C.A. Mirkin, *Angew. Chem. Int. Ed.*, 2007, **46**, 4093-4096, doi: 10.1002/anie.200700269.

[13] J. Hu, J. Li, J. Qi and J. Chen, *New J. Chem.*, 2015, **39**, 843–848, doi:10.1039/C4NJ01147C.

[14] A. Shafawi, L. Ebdon, M. Foulkes, P. Stockwell and W. Corns, *Analyst*, 1999, **124**, 185–189, doi: 10.1039/A809679A.

[15] I.L.S. Almeida and N.M.M. Coelho, *Energy Fuels*, 2012, **26**, 6003–6007, doi:10.1021/ef3010042.

[16] J.C. Yu, J.M. Lo and C.M. Wai, *Anal. Chim. Acta*, 1983, **154,** 307–312, doi:10.1016/0003-2670(83)80032-4.

[17] M.J. Powell, E.S.K. Quan, D.W. Boomer and D.R. Wiederin, *Anal. Chem.*, 1992, **64**, 2253–2257, doi: 10.1021/ac00043a012.

[18] P. Ugo, L.M. Moretto, P. Bertoncello, J. Wang, *Electroanalysis*, 1998, **10**, 1017–1021, doi: 10.1002/(SICI)1521-4109(199810)10:15%3C1017::AID ELAN1017%3E3.0.CO;2-D.

[19] S.Y. Lee, J. J. Lee, K. H. Bok, J. A. Kim, S.Y. Kim and C. Kim, *Inorg. Chem. Commun.*, 2016, **70**, 147–152, doi: 10.1016/j.inoche.2016.06.004.

[20] C.G. Lee, S. Kang, J. Oh, M. S. Eom, J. Oh, M-G Kim, W. S. Lee, S. Hong and M. S. Han, *Tetrahedron Lett.*, 2017, **58**, 4340–4343, doi: 10.1016/j.tetlet.2017.09.082.

[21] M.Z. Jonaghani and H. Zali-Boeini, *Spectrochim. Acta A*, 2017, **178**, 66–70, doi: 10.1016/j.saa.2017.01.065.

[22] K. Velmurugan and R. Nandhakumar, *J. Lumin.*, 2015, **162**, 8–13, doi: 10.1016/j.jlumin.2015.01.039.

[23] T.D. Giacco, R. Germani, F. Purgatorio and M. Tiecco, *J. Photochem. Photobio. A*, 2017, **345**, 74–79, doi: 10.1016/j.jphotochem.2017.05.032.

[24] A.K. TG, V. Tekuri, M. Mohan and D.R. Trivedi, *Sens Actuators B Chem.*, 2019, **284,** 271-280, doi: 10.1016/j.snb.2018.12.003.

[25] B.K. Momidi, V. Tekuri and D.R. Trivedi, Inorg. *Chem. Commun.*, 2016, **74**, 1–5, doi: 10.1016/j.inoche.2016.10.017.

[26] J. Liu, M. Yu, X.C. Wang and Z. Zhang, *Spectrochim. Acta A*, 2012, **93**, 245–249, doi: 10.1016/j.saa.2012.03.021.

[27] R. Kavitha and T. Stalin, *J. Lumin*, 2014, **149**, 12–18, doi: 10.1016/j.jlumin.2013.11.044.

[28] E. Ermakova, J. Michalak, M. Meyer, V. Arslanov, A. Tsivadze, R. Guilard and A. Bessmertnykh-Lemeune, *Org. Lett.*, 2013, **15**, 662–665, doi: 10.1021/ol303499v.

[29] Z. Yan, M-F Yuen, L. Hu, P. Sun and C-S Lee; *RSC Adv.*, 2014, **4,** 48373-48388, doi: 10.1039/C4RA07930B.

[30] D. Li, C-Y Li, Y-F Li, Z. Li and F. Xu, *Anal. Chim Acta*, 2016, **934,** 218-225, doi:10.1016/j.aca.2016.05.050.

[31] M. Bahta and N. Ahmed, *J. Photochem. Photobio. A*, 2019, **378**, 85–93, doi: 10.1016/j.jphotochem.2019.04.027.

[32] Y. Fang, X. Li, J-Y Li, G-Y Wang, Y. Zhou, N-Z Xu, Y. Hu and C. Yao *Sens. Actuators B Chem.*, 2018, **255**, 1182–1190, doi: 10.1016/j.snb.2017.06.050.

[33] X-C Liang, S. Chen, J. Gao, H. Zhang, Y. Wang, J-Hu Wang and L. Feng, *Sens. Actuators B Chem.*, 2018, **265**, 293–301, doi: 10.1016/j.snb.2018.01.182.

[34] S. K. Sharma, N. Kaur, J. Singh, A. Singh, P. Raj, S. Sankar, D. Y. Kim, N. Singh, N. Kaur and H. Singh, *Sens. Actuators B Chem.*, 2016, **232,** 712–721, doi: 10.1016/j.snb.2016.04.017.

[35] W-J Qu, G-Y Gao, B-B Shi, T-B Wei, Y-M Zhang, Q. Lin and H. Yao, *Sens. Actuators B Chem.*, 2014, **204**, 368–374, doi: 10.1016/j.snb.2014.07.101.

[36] L. Feng and Z. Chen, *Sens. Actuators B Chem.*, 2007, **122**, 600–604, doi: 10.1016/j.snb.2006.07.007.

[37] P. Wang, L. Zhao, H. Shou, J. Wang, P. Zheng, Kun Jia and X. Liu, *Sens. Actuators B Chem.*, 2016, **230**, 337–344, doi: 10.1016/j.snb.2016.02.041.

[38] Q. Zhang, J. Zhang, H. Zuo, C. Wang and Y. Shen; *Tetrahedron*, 2017, **73**, 2824-2830, doi: 10.1016/j.tet.2017.03.088.

[39] M. Suresh, M. Mishra, S.K. Mishra, E. Suresh, A.K. Mandal, A. Shrivastav and A. Das, *Org. Lett.*, 2009, **11**, 2740–2743, doi: 10.1021/ol900810q.

[40] H-S Kim, S. Angupillai, Y-M Jeong, J-S Park, C-H Kim and Y-A. Son *Sens. Actuators B Chem.*, 2017, **240**, 1272–1282, doi: 10.1016/j.snb.2016.09.115.

[41] A.P. de Silva, H.Q.N. Gunaratne, P. L. M. Lynch, A. J. Patty and G. L. Spence, *J. Chem. Soc., Perkin Trans. 2*, 1993, 1611-1616, doi: 10.1039/P29930001611.

[42] L. Fabbrizzi and A. Poggi, *Chem. Soc. Rev*. 1995, **24**, 197-202, doi:10.1039/CS9952400197.

[43] D. J. Cram, *Angew. Chem., Int. Ed. Engl*. 1988, **27**, 1009-1020, doi: 10.1002/anie.198810093.

[44] P. Gosavi-Mirkute, A. Patil, D. N. Lande, D. Chakravarty, S. P. Gejji, S. Satpute and S. Salunke-Gawali, *RSC Adv*., 2017, **7**, 55163-55174, doi: 10.1039/C7RA10490A.
[45] A. P. Ware, A. Patil, S. Khomane, T. Weyhermuller, S. S. Pingale and S Salunke-Gawali, *J Mol. Struct.*, 2015, **1093**, 39-48, doi: 10.1016/j.molstruc.2015.03.016.
[46] A. Patil, A. P. Ware, S. Bhand, D. Chakravarty, R. Gonnade, S. S. Pingale and S Salunke-Gawali, *J Mol. Struct.*, 2016, **1114**, 132-143, doi: doi: 10.1016/j.molstruc.2016.02.065.
[47] A. Patil, D. N. Lande, A. Nalkar, S. P. Gejji, D. Chakravarty, R. Gonnade, T. Moniz, M. Rangel, E. Pereira and S Salunke-Gawali, *J Mol. Struct.*, 2017, **1143**, 495-514, doi: 10.1016/j.molstruc.2017.04.094.
[48] S. Madhupriya and K.P. Elango, *Spectrochim. Acta A*, **2012**, **97**, 100-104. doi: 10.1016/j.saa.2012.05.044.
[49] S. Madhupriya and K.P. Elango, *Spectrochim. Acta A*, 2012, **97**, 429-434. doi: 10.1016/j.saa.2012.06.020.
[50] C. Parthiban, R. Manivannan and K. P. Elango, *Dalton Trans.*, 2015, **44**, 3259-3264. doi: 10.1039/C4DT03289F.
[51] R. H. Thomson, Naturally Occurring Quinones IV. Recent Advances, 4th ed., Blackie Academic & Professional: London, 1997.
[52] P. E. Cockram and T. K. Smith, *J. Nat. Prod.*, 2018, **81**,2138-2154, doi:10.1021/acs.jnatprod.8b00159.
[53] Z. G. Ding, J. Y. Zhao, M. G. Li, R. Huang, Q. M. Li, X. L. Cui, H. J. Zhu, and M. L. Wen, *J. Nat Prod.*,2012, **75**, 1994-1999, doi: 10.1021/np3004936.
[54] C. C. Nawrat, L. I. Palmer, A. J. Blake and C.J. Moody, *J. Org. Chem.*, 2013, **78**, 5587-5603, doi: 10.1021/jo400737f.
[55] Y. Kumagai, Y. Shinkai, T. Miura, and A. K. Cho, *Annu. Rev. Pharmacol. Toxicol.*, 2012, **52**, 221-247, doi: 10.1146/annurev-pharmtox-010611-134517.
[56] J. Li, C. Jiao, K-W. Huang and J. Wu, *Chem. Eur. J.*, 2011, **17**, 14622-14680. doi:10.1002/chem.201102120.
[57] Y. C.Hao Jiang, L. Zhengtao, N. Wu, Z. Yang, and J. Quan, *Org. Lett.*, 2009, **11**, 4628-4631, doi: 10.1021/ol901902v.
[58] J. Sperry, J. J. P. Sejberg, F. M. Stiemke, and M. A. Brimble, *Org. Biomol. Chem.*, 2009, **7,** 2599-2603, doi:10.1039/b905077a.
[59] H. J. Banks, D. W. Cameron, M. J. Crossley and E. L. Samuel, *Aus. J. Chem.*, 1976, **29**, 2247-2256, doi: 10.1071/ch9762247.
[60] A. V. Bogdanov, N. R. Khasiyatullina, V. F. Mironov, D. B. KrivolapovIgor, A. Litvinov and A. I. Konovalov, *Mendeleev Commun.*, 2009, **19**, 39-41, doi: 10.1016/j.mencom.2009.01.016.
[61] J. Guo, Y. W. Xu, K. Li, L. M. Xiao, S. Chen, K. Wu, X. D. Chen, Y. Z. Fan, J. M. Liu and C. Y. Su, *Angew. Chem. Int. Ed.*, 2017, **56**, 3852-3856, doi:10.1002/anie.201611875.
[62] D. Chadar, S. S. Rao, S. P. Gejji, B. Ugale, C. M. Nagaraja, M. Nikalje and S. Salunke-Gawali**,** *RSC Adv.*, 2015, **5**, 76419-76423, doi:10.1039/C5RA13169C.
[63] G. Agarwal, D. N. Lande, D. Chakravarty, S. P. Gejji, P. Gosavi-Mirkute, A. Patil and S. Salunke-Gawali, *RSC Adv.*, 2016, **6**, 88010-88029, doi: 10.1039/C6RA20970J.
[64] D. D. Perrin, W. L. Armarego and D. R. Perrin, Purification of Laboratory Chemicals, 2nd Edn., Pergamon Press, Oxford, 1988, p. 260.
[65] Bruker, APEX2, SAINT and SADABS: Bruker AXS Inc., Madison, Wisconsin, USA. 2007.
[66] G. M. Sheldrick, *Acta Crystallogr. A*, 2008, **A64**, 112-122, doi: 10.1107/S0108767307043930.
[67] C. F. Macrae, I. J. Bruno, J.A. Chisholm, P. R. Edgington, P. McCabe, E. Pidcock, L. Rodriguez-Monge, R. Taylor, J. van de Streek and P. A. Wood, *J. Appl. Crystallogr.*, 2008, **41**, 466-470, doi:10.1107/S0021889807067908.
[68] A. L. Spek, *Acta Crystallogr*., 2009, **D65**, 148-155, doi:10.1107/S090744490804362x.
[69] J. D. Chai and M. Head-Gordon, *J. Chem. Phys.*, 2008, **128**, 084106,doi: 10.1063/1.2834918.
[70] M. J. Frisch, G. W. Trucks, H. B. Schlegel, G. E. Scuseria, M. A. Robb, J. R. Cheeseman, J. A. Montgomery Jr, T. Vreven, K. N. Kudin, J. C. Burant, J. M. Millam, S. S. Iyengar, J. Tomasi, V. Barone, B. Mennucci, M. Cossi, G. Scalmani, N. Rega, G. A. Petersson, H. Nakatsuji, M. Hada, M. Ehara, K. Toyota, R. Fukuda, J. Hasegawa, M. Ishida, T. Nakajima, Y. Honda, O. Kitao, H. Nakai, M. Li, X. Klene, J. E. Knox, H. P. Hratchian, J. B. Cross, V. Bakken, C. Adamo, J. Jaramillo, R. Gomperts, R. E. Stratmann, O. Yazyev, A. J. Austin, R. Cammi, C. Pomelli, J. W. Ochterski, P. Y. Ayala, K. Morokuma, G. A. Voth, P. Salvador, J. J. Dannenberg, V. G. Zakrzewski, S. Dapprich, A. D. Daniels, M. C. Strain, O. Farkas, D. K. Malick, A. D. Rabuck, K. Raghavachari, J. B. Foresman, J. V. Orti, Q. Cui, A. G. Baboul, S. Clifford, J. Cioslowski, B. B. Stefanov, G. Liu, A. Liashenk, P. Piskorz, I. Komaromi, R. L. Martin, D. J. Fox, T. Keith, M. A. Al-Laham, C. Y. Peng, A. Nanayakkara, M. Challacombe, P. M. W. Gill, B. Johnson, W. Chen, M. W. Wong, C. Gonzalez and J. A. Pople, Gaussian, revision, C.01,Wallingford, CT: Gaussian, Inc. 2004.
[71] G. A. Petersson, T. G. Tensfeldt and J. A. Montgomery Jr, *J. Chem. Phys.*, 1991, **94**, 6091, doi:10.1063/1.460448.
[72] S. Salunke-Gawali, O. Pawar, M. Nikalje, R. Patil, T. Weyhermüller, V. G. Puranik and V. B. Konkimalla, *J. Mol. Struct.*, 2014, **1056-1057**, 97-103, doi: 10.1016/j.molstruc.2013.10.016.
[73] U. A. Dar, S. Bhand, D. N. Lande, S. S. Rao, Y. P. Patil, S. P. Gejji, M. Nethaji, T. Weyhermüller and S. Salunke-Gawali, *Polyhedron*, 2016, **113**, 61-72, doi: 10.1016/j.poly.2016.04.002.
[74] D. Choudhari, D. Chakravarty, D. N. Lande, S. Parveen, S.P. Gejji, K. M. Kodam and S. Salunke-Gawali, *Struct. Chem.*, 2019, **30**, 2257-2270, doi: 10.1007/s11224-019-01343-8.
[75] S. Salunke-Gawali, E. Pereira, U. A. Dar and S. Bhand, *J. Mol. Struct.*, 2017, **1148**, 435-458, doi: 10.1016/j.molstruc.2017.06.130.
[76] P. J. Gaultier and E. C. Hauw, *Acta Cryst.*, 1966, **20**, 620, doi: 10.1107/s0365110x66001518.
[77] P. J. Gaultier and E. C. Hauw, *Acta Cryst.*, 1969, **B25**, 419, doi: 10.1107/s0567740869002524.

Author information

Gunjan Aggrwal *completed her Ph.D. in 2020 under the guidance of Professor Sunita Salunke-Gawali at Savitribai Phule Pune University, Pune (India). She passed a National eligibility Test for Lectureship conducted by CSIR-UGC in 2010 and received her Master's degree in Inorganic Chemistry in 2004. Her research interests are synthesis of chemosensor ligands and transition metal complexes of naphthoquinone derivatives.*

Sunita Salunke-Gawali *She received her M.Sc.(1993) in Inorganic Chemistry and Ph.D. (1999) from Pune University. As a professional experience she worked as Post-doctoral Research Associate at Laboratoire de Magnétisme et d'Optique, Versailles France (Prof. F. Varret, 2001-2002), Department of Chemistry, IIT Bombay, India (Prof. C. P. Rao, 2002 and 2004), Universidade do Porto, Portugal, supervised by Prof. Eulália Pereira (2004-2007) and Max-Planck-Institut für Bioanorganische Chemie, Mülheim an der Ruhr, Germany (Dr. Eckhard Bill, 2007- 2008). She joined as Reader in Department of Chemistry, Savitribai Phule Pune University in 2008, where she serves as Professor. Her research interests include coordination and bioorganic Chemistry of naphthoquinone ligands, developing photosensitizer for DSSC, HPLC method development for anticancer drugs and separation of tautomers, chemosensors and metallosurfactants. She is the author of more than 87 articles in international journals.*

Shridhar P. Gejji *is the former head, department of Chemistry, Savitribai Phule Pune University, Pune, India. He received M. Sc. (in1980) and Ph. D. (in 1985) from the same university. He has professional experience in Theoretical and Computational Chemistry from the Institute of Quantum Chemistry and Department of Inorganic Chemistry, Uppsala University, Sweden (1987-1994). His academic positions include Reader (1995-2003) and Professor of Physical Chemistry (2003-2018). He continues to be emeritus Professor at the department of Chemistry, Savitribai Phule Pune University, India. He has authored more than 160 articles in the International Journals.*

Milind Nikalje *received M. Sc. (in1994) in Organic Chemistry from University of Pune and Ph. D. (in 2002) from National Chemical Laboratory, Pune. He has professional experience as a JSPS fellow at GIFU University, Japan (2003-2005). He joined Savitribai Phule Pune University in 2002, and continues as Associate Professor in the same University. His research interest includes synthetic organic chemistry and asymmetric synthesis.*

Debamitra Chakravarty *completed her Master of Science from Bangalore University. She received her M. Phil. from Department of Zoology, Savitribai Phule Pune University, Pune (India) under the guidance of Dr. Deepti Deobagkar. She received training on X-ray crystallography at CSIR-National Chemical Laboratory under the guidance Dr. Vedavati G. Puranik. Later she worked as Instrument Operator of Single Crystal X- Ray Diffractometer at Central Instrumentation facility, Savitribai Phule Pune University. Her research interests are chemical crystallography and medicinal biology.*

Prakash L. Verma *completed his Ph.D. (2019) and M.Phil. (2015) degrees under guidance of Professor Shridhar P. Gejji from Savitribai Phule Pune University, Pune (India) in theoretical Chemistry. He received his master's in Physical Chemistry in 2010; he worked as Junior Research Fellow at IISER Bhopal, India.*

Mahesh Jadhav *is a Ph. D. student working under guidance of Professor Sunita Salunke - Gawali at Savitribai Phule Pune University, Pune (India). He received his M. Sc. in Analytical Chemistry in 2008, and M. Phil. degree in 2016. He worked in Centaur Pharmaceutical Pvt. Ltd. as junior officer in quality control (2008-2009). He also worked in National Chemical Laboratory (NCL) Pune as a project fellow (2010- 2013) in Chemical Engineering and Process Development department. Currently, he is working in Indian Institute of Science Education and Research (IISER) Pune as a Technical Officer since 2013. His research interests are*

synthesis of naphthoquinone ligands and their metal complexes for energy harvesting and storage application.

Prajakta Gosavi-Mirkute *is Ph. D. student under the guidance of Prof. Sunita Salunke-Gawali at Savitribai Phule Pune University, Pune (India). She received her master's degree in Organic Chemistry in 2014 and M.Phil. in 2018. Her research interest includes first row transition metal ion detection by naphthoquinone and anthraquinone based chemosensors.*

Shital Harihar *is a Ph.D. student under the guidance of Professor Sunita Salunke-Gawali at Department of Chemistry, Savitribai Phule Pune University. She received her Master's degree in Inorganic Chemistry in 2016 from the same university. She qualified the State Eligibility Test (SET 2018) for Assistant Lecturership. Her research interests are Synthesis, characterization and of biological activity naphthoquinone metal.*

Vedavati G. Puranik*, Educated from Bangalore University India and later on worked at National Chemical Laboratory, Pune as senior scientist from 1983. Executive committee member for Indian crystallographic Association. Invited talk at Universität Leipzig Fakultät für Chemie und Mineralogie, Institut für Anorganische Chemie, Leipzig, at Korea Research Institute of Chemical Technology (KRICT) Daejon, at different Pharmaceutical companies, R & D institutes, at various colleges and university in Pune and other states of India. Consultancy for dfferent Pharma Industries. Refereed many manuscripts of different international journals. Visited Parry Sound, Ontario, Canada for International Conference on Bioinorganic Chemistry, Institut für Anorganische Chemie, Christian-Albrechts Universität Kiel, Germany, for DST_DAAD project. Member for The International Associate Laboratories programe (2013-16) between NCL, CNRS and Unité de Catalyse et de Chimie du Solide (UCCS), France. She is the author of more than 270 articles in international journals. Research interests are single crystal X-ray analysis different compounds, bioactive molecules from natural sources and Chemically Synthesised novel anticancer compounds and structure activity correlations.*